



31 Due to its high porosity, planting concrete as plant bedding has been evaluated as an economical and  
32 environmentally friendly alternative to traditional impervious hard concrete for the purpose of growing  
33 plants, conserving water and soil [8]. Generally, planting concrete consists of cementitious materials,  
34 coarse aggregate, water and admixtures. Among the components, cementitious material directly  
35 determines the water absorption capacity, the water and fertilizer retention capacities, the alkalinity and  
36 other relevant properties, making it indisputably one of the most important components of planting  
37 concrete.

38 The cementitious material can be divided into two main types: Portland cement (PC) and SAC-based  
39 cementitious materials. The major hydration products of PC are C-S-H and calcium hydroxide (CH)  
40 [9-11], while AFt ( $C_3A \cdot 3C\$\cdot H_{32}$ ; C = CaO, A =  $Al_2O_3$ , \$ =  $SO_3$ , H =  $H_2O$ ) and AFm ( $C_3A \cdot C\$\cdot H_{12}$ ) are  
41 the main principle crystal products during the hydration of SAC [12-14]. Therefore the alkalinity of  
42 pore fluid of hydrated SAC is lower than PC [15-18], making it a favourable environment for plant  
43 growth. In addition, the production of SAC has the advantage of a lower calcination temperature  
44 ( $\sim 1250^\circ C$ ), lower  $CO_2$  emissions and easier grinding with less energy required [19-24]. Furthermore,  
45 using SAC can shorten the construction period due to its rapid hardening and high strength gain  
46 [25-27]. Therefore, the use of SAC is more suitable as a cementitious material compared with OPC.

47 But the water absorption capacity, water and fertilizer retention properties of the hardened paste of  
48 traditional cementitious material still cannot meet plant growing demand. Plants living in planting  
49 concrete can often wither and die, defeating the primary purpose of a planting concrete. On the other  
50 hand, vermiculite has a high water absorption capacity and desirable water retention capacity [28]. The  
51 study of Kiyoshi Okada et al. observed that mixing allophane with vermiculite could control various  
52 pore sizes, which was a very good strategy for enhancing the water retention capacity of planting  
53 concrete [28, 29]. Vermiculite is a hydrous phyllosilicate mineral consisting of a 2:1 layered structure,  
54 and possesses the ability to store water molecules and exchangeable cations in its interlayer space  
55 [30-32]. Each layer in vermiculite consists of octahedrally coordinated cations (typically Mg, Al  
56 and Fe) about 1 nm in thickness, sandwiched by tetrahedrally coordinated cations (typically Si and  
57 Al) [33, 34]. The interlayer space of vermiculite is characterized by adsorption, ion exchange, etc. [31].  
58 According to the basic theory of 'fertilizer moves with water' [35, 36], vermiculite also has a desirable  
59 fertilizer retention capacity. So it was evident that vermiculite is suitable to improve the water  
60 absorption capacity, water/fertilizer retention properties of cementitious materials.

61 Therefore, in this paper, vermiculite was adopted to partially replace SAC in order to prepare a  
62 cementitious material with an enhanced water absorption capacity, water/fertilizer retention properties.  
63 At the same time, urea was adopted as the fertilizer to study the effect of vermiculite on the fertilizer  
64 retention property of SAC-based material. Another important intention of this study is to determine  
65 vermiculite's effect on the basic physicochemical properties and the mechanisms, such as alkalinity of  
66 pore fluid, pore structure, mechanical properties, thermo-gravimetric analysis and heat of hydration.  
67 The intention of this paper is to offer useful data to advance the knowledge in the planting concrete  
68 industry, especially for cementitious material.

## 69 **2. Materials and Methods**

### 70 **2.1 Materials**

71 SAC (42.5 R, manufactured in China) was used as the base cementitious material in this study, whose  
72 initial and final setting times were 15 min and 21 min, respectively. The exfoliated vermiculite from a  
73 local supplier, calcined at 850°C. The chemical compositions of SAC and vermiculite were determined  
74 by X-ray fluorescence spectrometer (Tiger S8, Bruker AXS GMBH, Germany), and are given in Table  
75 1. Particle size distributions of SAC and vermiculite were determined using a laser particle size  
76 analyzer (LS13320, Beckman, USA) and are presented in Fig.1.

77 Urea (with a purity of 99.0 wt.%, from Damao Chemical Reagent Factory, China) was adopted as  
78 fertilizer in this study. The urea was composed of no more than 0.005 wt.% water-insoluble substances,  
79 had an ignition loss of no higher than 0.01 wt.%, and a burette content of no more than 0.2wt. %.

### 80 **2.2 Experimental design**

81 In this study, vermiculite was used to partially replace SAC at the replacement levels of 5%, 10%, 20%  
82 and 40% by weight and marked as SV 5, SV 10, SV 20 and SV 40, respectively. A control sample of  
83 SAC without vermiculite was named SV ref. The mix proportions of the investigated SAC-based  
84 cementitious materials are shown in Table 2.

### 85 **2.3 Sample preparation**

86 The pastes without fertilizer were prepared with a water-to-binder (W/B) weight ratio of 0.35, then cast  
87 in  $20 \times 20 \times 20$  mm<sup>3</sup> moulds and vibrated to remove air bubbles. The moulded pastes were kept in a  
88 curing environment of 20±2°C and 95+% RH. After 24 hours, the specimens were demoulded and then  
89 placed in water at 20±2 °C for 2 days. Subsequently, the hydration of the cement pastes was stopped by  
90 leaving samples immersed in absolute ethyl alcohol for 24h.

91 The pastes containing fertilizer were prepared and cured in the exact same conditions as described  
92 above, differentiating only in that fertilizer had been predissolved in the mixing water. The fertilizer  
93 contents used were 2%, 4% and 8% (by weight) of binder.

94 In this paper, mortars were adopted to study the mechanical property of cementitious materials, which  
95 were prepared and cured according to the Chinese National Standard GB 20472-2006 [37].

## 96 **2.4 Test methods**

### 97 2.4.1 Water absorption capacity

98 The water absorption capacities of the hardened pastes were tested at  $35\pm 2^\circ\text{C}$ . The hardened pastes  
99 without fertilizer were cured for 3 days followed by drying at  $35\pm 2^\circ\text{C}$  for 24h, after which they were  
100 accurately weighted and the mass recorded as  $m_0$ . Specimens were soaked in deionized water until the  
101 weight did not increase more than 0.1%. Samples were taken out from water and the surface water of  
102 the samples was gently dried to remove. Then the samples were accurately weighted and the mass was  
103 recorded as  $m_1$ . The Water Absorption Rate (WAR) of a sample was calculated as  
104  $\text{WAR} = [(m_1 - m_0) / m_0] \times 100\%$ .

### 105 2.4.2 Water retention property

106 The samples after the water absorption test were exposed to an environment of  $35\pm 2^\circ\text{C}$  and  $20\pm 2\%$  RH.  
107 At predetermined times (0.5h, 1h, 2h, 4h, 6h, 8h, 10h, 15h, 20h, 25h, 30h, 40h, ..., 80h, 100h, 120h),  
108 the samples were accurately weighed and the mass recorded as  $m_2$ . The water release rate (WRR) of a  
109 sample was calculated as  $\text{WRR} = [(m_1 - m_2) / (m_1 - m_0)] \times 100\%$ .

### 110 2.4.3 Fertilizer retention capacity

111 The hardened pastes' fertilizer retention capacity is demonstrated by fertilizer release rate in deionised  
112 water. Every sample was soaked in 100ml deionized water. At predetermined times (1d, 2d, ..., 7d,  
113 10d, 14d, 21d, 28d, 35d), the fertilizer concentration of the soaking solution was tested by  
114 ultraviolet-visible spectroscopy (UV-VIS) [38]. After each test, the soaking water was replaced by  
115 another 100ml pure deionised water.

### 116 2.4.4 Alkalinity of pore fluid

117 For this test, ex-situ leaching [39] was adopted to prepare the pore liquid. The pH was tested by using a  
118 laboratory grade pH meter (Spsic, PHS-3E, China).

### 119 2.4.5 TG-DSC analysis

120 TG-DSC analysis was conducted to estimate quantitatively the hydration product content, especially

121 the CH content using a simultaneous thermal analyzer (Mettler, TGA/DSC1/1600HT, Sweden) at a  
122 heating rate of 20°C/min from 0°C to 800°C under argon atmosphere.

#### 123 2.4.6 Mechanical properties

124 The mechanical properties of the samples were tested according to the Chinese National Standard  
125 GB20472-2006[37].

#### 126 2.4.7 Hydration heat evolution

127 A conduction calorimeter (TAM Air C80, Thermometric, Sweden) operating at 25°C was used to  
128 determine the hydration heat flow. For such purpose, a water to binder of 0.5 was adopted, and the heat  
129 flow was recorded every 44s until 72h.

#### 130 2.4.8 Bulk density

131 The bulk density of hardened paste specimens was measured by the water vacuum saturation method  
132 [40, 41]. The specimens were dried at 65°C in order to remove the majority of the physically bound  
133 water. After that, the hardened pastes were placed into a desiccator with deaired water. For the duration  
134 of three hours, air was evacuated with a vacuum pump from the desiccator. The hardened pastes were  
135 then kept in water for more than 24h.

#### 136 2.4.9 Pore structure

137 Mercury intrusion porosimetry was employed to examine the pore structure of hardened pastes. An  
138 automatic mercury porosimetry (Pore Master-60, Quanta- chrome Instruments, USA) was used in this  
139 study, whose intrusion accuracy was  $\pm 0.11\%$ .

### 140 **3. Results and Discussion**

#### 141 **3.1 Planting potential**

##### 142 3.1.1 Water absorption capacity

143 The WARs of hardened pastes are shown in Table 3. The WAR of SV ref was only 8.05wt.%. When the  
144 dosage of vermiculite was 5 wt.%, the WAR increased by 16.8% to a value of 9.40 wt.%. Evidently,  
145 with the increase of vermiculite dosage, the WAR increased. This trend continued with the increase of  
146 vermiculite dosage. With an addition of 20 wt.% vermiculite, the WAR reached up to 14.82 wt.%, an  
147 increase of 84.1% compared to the SV ref. Therefore vermiculite proved to be suitable to improve the  
148 water absorption capacity of cementitious material pastes.

##### 149 3.1.2 Water retention capacity

150 The measured water release rates of hardened pastes are presented in Fig.2, representing their water

151 retention capacity. When the exposure time was less than 8h, the water release rate of pastes increased  
152 with the increasing of vermiculite dosage. A possible reason was that with the increase of vermiculite  
153 dosage, the open porosity at sample surfaces increased, resulting the amount of free water at sample  
154 surfaces to increase. The water release rate of SV ref reached up to 98.9% at 120h. At the same time,  
155 the water release rate of SV 20 was only 80.4%, suggesting that vermiculite could improve water  
156 retention capacity of cementitious pastes. This enhancement can be attributed to the increased internal  
157 porosity imparted by vermiculite.

### 158 3.1.3 Fertilizer retention capacity

159 The fertilizer release rates from hardened pastes are presented in Fig.3, which represent the fertilizer  
160 retention property. The fertilizer release rates increased with the increase of soaking time. The fertilizer  
161 release rate of SV ref at 35d was highest and reached up to 96.3 wt.% when fertilizer dosage was 20 wt.%  
162 (Fig.3 (a)), suggesting that the fertilizer added during mixing could be released slowly in the hardened  
163 pastes. And the fertilizer release rate grew with a straight-line at early ages (i.e. up to 7d) and with the  
164 further extending of soaking time the curves of fertilizer release rate became flatten, indicating that the  
165 velocity of fertilizer release decreased with the increase of soaking time.

166 In this study, in cases of a vermiculite content of less than 20wt.%, the fertilizer release rate from  
167 hardened pastes decreased with the increase of vermiculite content at the same soaking times. For  
168 example, in Fig.3(b) the 35d fertilizer release rate of SV 5, SV10 and SV 20 were 62.9 wt.%, 60.2 wt.%  
169 and 54.3 wt.% lower than that of SV ref. However, 40 wt.% vermiculite could increase the fertilizer  
170 release rate of hardened pastes compared with SA ref with 0 wt.% vermiculite, which suggests that  
171 excessive vermiculite is not beneficial to the fertilizer retention property of cementitious materials.  
172 Therefore vermiculite dosage should be less than 20 wt.%, which could improve the fertilizer retention  
173 capacity of an SAC-based cementitious material.

174 In addition, there was a phenomenon worthy noting here. When using a fertilizer dosage of 8 wt.% at  
175 most, for the same kind of materials, the fertilizer release rates decreased with the increase of fertilizer  
176 addition. Therefore, a proper fertilizer dosage could also improve the fertilizer retention property of  
177 cementitious materials.

### 178 3.1.4 Alkalinity

179 Fig.4 shows the alkalinity of pore fluid of hardened cementitious pastes. A previous study [42]  
180 demonstrated that the pH of pore fluid of hardened PC paste was about 13 as determined by ex-situ

181 leaching. In this study, the pH of pore fluid of SV ref was 11.40, which is significantly less than that of  
182 PC. The pH of pore fluid of the hardened pastes decreased gradually with the increase of vermiculite  
183 dosage, and the pH of SV 20 and SV 40 was measured to be 10.95 and 10.71, respectively. Therefore,  
184 vermiculite could effectively reduce the alkalinity of pore fluid of hardened SAC-based materials. This  
185 result further proves that SAC-based cementitious materials with vermiculite are suitable to prepare  
186 planting concrete.

187 The TG-DSC analyses of the hydration products are shown in Fig.5. The TG-DSC curves (Fig.5 (a)) of  
188 SV 20 and SV 40 became gentler compared with that of SV ref. at 400°C~500°C which was the  
189 decomposition temperature of CH [43]. According to TG-1st derivative curve (Fig.5 (b)), the area of  
190 the endothermic peak of SV ref was less than that of SV ref at 400°C~500°C and no corresponding  
191 peak was seen in that of SV 40. These suggested that the CH content of hardened pastes was decreased  
192 by vermiculite. As increased amounts of SAC were replaced by vermiculite, this reduced the amount of  
193 CH that could potentially form from the hydration of SAC.

194 Furthermore, the total pore volume and pore liquid content increased with the increase of vermiculite  
195 dosage, which decreased the concentrations of  $\text{Ca}^{2+}$  and  $\text{OH}^-$  of pore fluid of hardened pastes. The  
196 formation and growth of CH crystals were limited. Therefore, the alkalinity of pore fluid of hardened  
197 pastes decreased with the increase of vermiculite content. Therefore, it was concluded that vermiculite  
198 played a positive role during the hydrating of the cementitious materials to reduce alkalinity. Low  
199 alkalinity was helpful for plant growing in planting concrete and achieved the expected value in this  
200 study.

## 201 **3.2 Basic physicochemical properties**

### 202 3.2.1 Mechanical properties

203 The mechanical properties of SAC-based cementitious materials are presented in Fig.6. The  
204 compressive strength (Fig.6 (a)) and flexural strength (Fig.6 (b)) decreased with the increase of  
205 vermiculite dosage. The 1d, 3d and 28d compressive strength of SV ref reached up to 38.1, 45.5 and  
206 51.5 MPa, respectively and the 1d, 3d and 28d flexural strength reached up to 5.9, 7.8 and 8.1 MPa,  
207 respectively. For SV 5 at 1d, 3d, and 28d, the compressive strength was 36.5, 41.5 and 48.7 MPa,  
208 respectively, while flexural strengths of 5.6, 7.5, and 7.7 MPa, respectively, was attained at the same  
209 curing ages. So there was minor effect of 5 wt.% vermiculite on mechanical property of SAC-based  
210 materials. The 1d and 3d compressive strength of SV 20 were 28.5 and 35.1 MPa, respectively.

211 Compared to SV ref, the 1d and 3d compressive strength of SV 20 reduced 25.2% and 22.9%,  
212 respectively. Furthermore, the 3d compressive and flexural strength of SV 40 reduced to 19.4 and 4.1  
213 MPa, respectively. The 3d compressive strength and flexural strength of SV 40 reduced 57.4% and 47.4%  
214 compared with the corresponding value of SV ref. Therefore, a dosage of 40 wt.% vermiculite was very  
215 negative to the mechanical property of SAC-based materials.

### 216 3.2.2 Hydration heat evolution

217 Fig.7 shows the hydration heat evolution of SAC-based cementitious materials. There was minor effect  
218 of vermiculite addition on the first exothermic peak (heat of dissolution, the age of about 0.1h) of  
219 SAC-based materials. The second exothermic peak (the age of about 1h) decreased with the increase of  
220 vermiculite content, which was caused by the hydration of ye'elite ( $C_4A_3\$$ ) and the main hydration  
221 product was Aft ( $C_4A_3\$ + 2C\$ + 38H \rightarrow C_3A \cdot 3C\$ \cdot H_{32} + 2AH_3$ ). The third exothermic peak (at the age  
222 between 2 and 5h) was  $C_4A_3\$$  hydrate which produces Aft ( $C_4A_3\$ + 2C\$ + 38H \rightarrow C_3A \cdot 3C\$ \cdot H_{32} +$   
223  $2AH_3$ ), and the time between the second and the third exothermic peak became gradually longer with  
224 the increase of vermiculite dosage. The delay of the onset of the third peak has been considered as the  
225 induction period of the hydration of  $C_4A_3\$$ . Therefore, it can be concluded that vermiculite can increase  
226 the induction period of the hydration of  $C_4A_3\$$ . Presumably, it was caused by the increased water  
227 absorption by vermiculite. In addition, the fourth exothermic peak (at the age about 5h), which  
228 represents the hydration of  $C_4A_3\$$  to produce AFm ( $C_4A_3\$ + 18H \rightarrow C_3A \cdot C\$ \cdot H_{12} + 2AH_3$ ), increased  
229 with the increase of vermiculite content.

230 Furthermore, the 1d and 3d cumulative heats of SV 5 and SV 10 were similar to those of SV ref. So  
231 there was negligible effects of 5 wt.% and 10 wt.% vermiculite content on the 1d and 3d cumulate heat  
232 of SAC-based materials. So 1d and 3d mechanical properties of SV 5 and SV 10 were similar to those  
233 of SV ref. In addition, the 1d and 3d cumulate heats of SV 20 were slightly lower than those of SV ref.  
234 Also, the 1d and 3d cumulate heats of SV 40 were significantly lower than those of SV ref. Therefore  
235 the 1d and 3d mechanical properties of SV 40 were significantly lower than those of SV ref. It was  
236 because that 40 wt.% SAC had been replaced by vermiculite.

### 237 3.2.3 Pore structure

238 The cumulative pore volumes of hardened pastes are shown in Fig.8. The total pore volume of SV ref  
239 was only 9.0%, which can be attributed to its poor water absorption capacity. The total pore volume  
240 increased with the increase of vermiculite dosage, which was probably due to the difference in the



241 particle size between SAC and vermiculite (Fig.1). Hence the water absorption capacity increased with  
242 the increase of vermiculite dosage. Compared to SV ref, the total pore volume of SV 10 and SV 20  
243 increased by 31.1% and 66.7%, respectively. Therefore, vermiculite was able to improve the total pore  
244 volume of hardened SAC-based pastes.

245 Fig.9 presents the pore size distribution of hardened pastes. While the vermiculite content was no more  
246 than 20 wt.%, the increase of pore volume was mainly due to fine pores between 0.4 and 1 $\mu$ m in  
247 diameter. Generally, the water retention property can be enhanced by various pore sizes [29]. Therefore,  
248 the water retention property was improved by vermiculite as long as the vermiculite dosage is no more  
249 than 20 wt.%. However with a vermiculite dosage of 40 wt.%, the volume of pores between 0.2~1 $\mu$ m  
250 in diameter decreased while the volumes of 10~30 $\mu$ m and 100~200 $\mu$ m pores significantly increased,  
251 which were harmful to the water/fertilizer retention property and mechanical performance. So  
252 vermiculite addition could cause pore volume and pore size changed. The latter results explain the  
253 change of water absorption capacity, water/fertilizer retention property and mechanical performance of  
254 hardened SAC pastes prepared with varying dosages of vermiculite.

255 The bulk densities of hardened pastes are shown in Fig.10. In this study, the bulk density of hardened  
256 pastes decreased with the increase of vermiculite. The bulk density of SV ref reached up to 1.86 g/cm<sup>3</sup>,  
257 while the bulk density of SV 20 was only 1.72 g/cm<sup>3</sup>. Compared to SV ref, the bulk density of SV 20  
258 reduced 7.5%. When the dosage of vermiculite reached to 40 wt.%, the bulk density of hardened pastes  
259 further reduced to 1.61 g/cm<sup>3</sup> and was 13.4% lower than that of SV ref. So, vermiculite was beneficial  
260 to decrease the bulk density of hardened pastes. In addition, these also probably suggested that the  
261 compactness of hardened pastes decreased with the increase of vermiculite dosage. In other words, the  
262 porosity of hardened pastes increased with the increase of vermiculite dosage.

263 The relationships between total pore volume, WAR and bulk density of hardened pastes are shown in  
264 Fig.11. The correlation coefficient between total pore volume and WAR reached up to 0.9981, which  
265 proved that there was an extremely significant linear correlation between them. Furthermore, the water  
266 absorption capacities of SV ref, SV 5, SV 10, SV 20 and SV 40 were 8.05wt.%, 9.40wt.%, 11.20wt.%,  
267 14.82wt.%, and 17.81wt.%, respectively. Water with a density of about 1g/cm<sup>3</sup> was used in all mixtures,  
268 so the water absorption capacities can be approximately expressed for SV ref, SV 5, SV 10, SV 20 and  
269 SV 40 as 0.081, 0.094, 0.112, 0.148 and 0.178 cm<sup>3</sup>/g, respectively. Additionally, the total pore densities  
270 of SV ref, SV 5, SV 10, SV 20 and SV 40 were 0.090, 0.102, 0.118, 0.150 and 0.175 cm<sup>3</sup>/g,

271 respectively. Therefore, the difference between water absorption and total pore volume decreased with  
272 the increase of vermiculite dosage. Those proved that the reason for the water absorption rate increased  
273 with the increase of vermiculite addition was not only due to the increase of pore volume, but  
274 vermiculite also has excellent water absorption property. Because vermiculite has 2:1 (tetrahedral–  
275 octahedral–tetrahedral) type layered structure, weak bond existed between the layers of vermiculite  
276 molecular structure. So water is able to enter the layers of vermiculite molecular structure.  
277 In addition, the correlation coefficient of total pore volume and bulk density of hardened pastes reached  
278 up to 0.9736. It proves that the bulk density decreasing with the increase of vermiculite dosage was  
279 because the total pore volume increased with the increase of vermiculite content once again.

280

#### 281 4. Conclusions

282 In this paper, from the basis of multiple perspectives, the effects of vermiculite on water/fertilizer  
283 retention and basic physicochemical properties of SAC-based materials were investigated. The main  
284 conclusions that can be drawn are as following:

285 (1) The water absorption capacity of hardened SAC-based materials increased with the increase of  
286 vermiculite dosage. The water absorption capacity was improved 81.8% using 20 wt.%  
287 vermiculite.

288 (2) The adoption of vermiculite proved to be suitable for the enhancement of the water retention  
289 property of SAC-based materials when its dosage is no more than 20 wt.%. At 120h, the water  
290 release rate decreased by 18.5% at 20 wt.% vermiculite replacement level.

291 (3) The change of the fertilizer retention property of SAC-based material was similar to that of water  
292 retention property, because ‘fertilizer moves with water’. 20 wt.% vermiculite in the SAC-based  
293 materials was the best therapy for improving fertilizer retention. For the latter cement  
294 replacement level, the fertilizer release rate at 35d reduced 15.3 wt.% and 12.1 wt.% when the  
295 fertilizer dosage was 2 wt.% and 4 wt.%, respectively.

296 (4) Vermiculite can decrease the pore fluid alkalinity of hardened SAC-based pastes. The alkalinity of  
297 pore fluid of hardened pastes reduced 0.45 at 20 wt.% vermiculite dosage, which is beneficial for  
298 plant growth.

299 (5) The compressive strength and flexural strength decreased with the increase of vermiculite dosage.  
300 However, the 3d compressive strength and 3d flexural strength of SV 20 reached up to 35.1 and

301 6.0MPa, respectively, which can meet the requirement for planting concrete.

302 (6) The total pore volume of hardened SAC-based materials increased with the increase of vermiculite.

303 The total pore volume increased 6% when 20wt.% vermiculite was incorporated. The increase of

304 pore volume was mainly due to vermiculites' fine pores of diameter between 0.4~1 $\mu$ m.

### 305 **Acknowledgments**

306 This work was supported by the National Natural Science Foundation of China through the grants of

307 NO.51302104 and NO.51472109, and Science and Technology Development Plan of Shandong

308 Province through the grant of NO.2014GZX208001. In addition, this work was also supported by the

309 Program for Scientific Research Innovation Team in Colleges and Universities of Shandong Province.

### 310 **Reference**

311 [1] M. Aamer Rafique Bhutta, K. Tsuruta, J. Mirza. Evaluation of high-performance porous concrete  
312 properties. *Constr and Build Mater.* 2012;31: 67–73.

313 [2] P. Sung-Bum , T. Mang. An experimental study on the water-purification properties of porous  
314 concrete. *Cem Concr Res.* 2004;34:177–184.

315 [3] K. Čosić, L. Korat , V. Ducman , I. Netinger. Influence of aggregate type and size on properties of  
316 pervious concrete. *Constr and Build Mater.* 2015;78: 69–76.

317 [4] H. K. Kim, H. K. Lee. Acoustic absorption modeling of porous concrete considering the  
318 degradation and shape of aggregates and void ratio. *J. Sound Vib.* 2010;329:866–879.

319 [5] A. S. Agar-Ozbek, J. Weerheijm, E. S. K. Breugel. Investigating porous concrete with improved  
320 strength: Testing at different scales. *Constr and Build Mater.* 2013;41:480-490.

321 [6] M. Tarnai, H. Mizuguchi. Design, construction and recent applications of porous concrete in Japan.  
322 In: *Proceedings of the JCI symposium on design, construction and recent applications of porous con-  
323 crete*, Japan Concrete Institute, Tokyo. 2004;4:1–10.

324 [7] M. A. R. Bhutta, N. Hasanah. Properties of porous concrete from waste crushed concrete (recycled  
325 aggregate). *Constr and Build Mater.* 2013;47:1243–1248.

326 [8] X. Yan, C. Gong, S. Wang, L. Lu. Effect of aggregate coating thickness on pore structure features  
327 and properties of porous ecological concrete. *Mag Concr Res.* 2013;65(1):1–8.

328 [9] Z. Keren, Z. Jin, G. Mulbah. Influences of phosphate tailings on hydration and properties of  
329 Portland cement. *Constr and Build Mater.* 2015;98:593–601.

330 [10] M. R. Meier, M. Sarigaphuti, P. Sainamthip, J. Plank. Early hydration of Portland cement studied  
331 under microgravity conditions. *Constr and Build Mater.* 2015;93:877–883.

332 [11] R. Kaminskas, V. Cesnauskas, R. Kubiliute. Influence of different artificial additives on Portland  
333 cement hydration and hardening. *Constr and Build Mater.* 2015;95:537–544.

334 [12] L. H. J. Martin, F. Winnefeld, C. J. Müller, B. Lothenbach. Contribution of limestone to the  
335 hydration of calcium sulfoaluminate cement. *Cem Concr Comp.* 2015;62:204–211.

336 [13] S. W. Tang, H. G. Zhu, et al. Hydration stage identification and phase transformation of calcium  
337 sulfoal- uminate cement at early age. *Constr and Build Mater.* 2015;75:11–18.

338 [14] M. Juenger, F. Winnefeld, J. Provis, J. Ideker. Advances in alternative cementitious binders. *Cem*  
339 *Concr Res.* 2011;41:1232–43.

340 [15] F. Winnefeld, B. Lothenbach. Hydration of Calcium Sulfoaluminate Cements—Experimental  
341 Findings and Thermodynamic Modelling. *Cem Concr Res.* 2010;40(8):1239–1247.

342 [16] S. Meimei, P. Purnell, I. Richardson. Microstructure of interface between fibre and matrix in  
343 10-year aged GRC modified by calcium sulfoaluminate cement. *Cem Concr Res.* 2015;76:20–26.

344 [17] A. Telesca, M. Marroccoli. A hydration study of various calcium sulfoaluminate cements. *Cem*  
345 *Concr Comp.* 2014;53:224–232.

346 [18] M. García-Maté, A. G. De la Torre. Hydration studies of calcium sulfoaluminate cements blended  
347 with fly ash. *Cem Concr Res.* 2013;54:12–20

348 [19] Z. Xiong, Z. Ming, Z. Yongjuan. Preparation and properties of self-pulverizing calcium  
349 sulfoaluminate cement. *Constr and Build Mater.* 2012;34:107–113.

350 [20] M. Marie, G. Jean-François, A. Jean. Improving the mechanical performance of high-grade slag  
351 cement by the addition of Portland cement and sulfoaluminate cement. *Constr and Build Mater.*  
352 2012;37:291–300.

353 [21] X. Dong, S. Wang, C. Gong, L. Lu. Effects of aggregate gradation and polymer modifiers on  
354 properties of cement-EPS/vitrified microsphere mortar. *Constr and Build Mater.* 2014; 73:255– 260.

355 [22] M. García-Maté, A. G. D. Torre. Hydration studies of calcium sulfoaluminate cements blended  
356 with fly ash. *Cem Concr Res.* 2013;54:12–20.

357 [23] M. Marie, G. Jean-François, A. Jean. Improving the mechanical performance of high-grade slag  
358 cement by the addition of Portland cement and sulfoalum- inate cement. *Constr and Build Mater.*  
359 2012;37: 291–300.

360 [24] S. Berger, G. Aouad. Leaching of calcium sulfoaluminate cement pastes by water at regulated pH  
361 and temperature: experimental investigation and modeling. *Cem Concr Res.* 2013;53:211–220.

362 [25] Y. Liao, X. Wei, G. Li. Early hydration of calcium sulfoaluminate cement through electrical  
363 resistivity measurement and microstructure investigations. *Constr and Build Mater.* 2011;25: 1572–  
364 1579.

365 [26] G. Bernardo, A. Telesca, G. L. Valenti. A porosimetric study of calcium sulfoaluminate cement  
366 pastes cured at early ages. *Cem Concr Res.* 2006;36:1042– 1047.

367 [27] R. Trauchessec, J. M. Mechling, et al. Hydration of ordinary Portland cement and calcium  
368 sulfoaluminate cement blends. *Cem Concr Comp.* 2015;56: 106–114.

369 [28] K. Okada, S. Matsui, T. Isobe, et al. Water-retention properties of porous ceramics prepared from  
370 mixtures of allophane and vermiculite for materials to counteract heat island effects. *Ceram Int.* 2008;  
371 34:345–350.

372 [29] M. Valášková, G. Simha Martynková, B. Smetana, S. Študentová. Influence of vermiculite on the  
373 formation of porous cordierites. *Appl Clay Sci* 2009;46: 196–201

374 [30] E. S. Pouya, H. Abolghasemi, et al. Batch adsorptive removal of benzoic acid from aqueous  
375 solution on to modified natural vermiculite: Kinetic, isotherm and thermodynamic studies. *J Ind Eng*  
376 *Chem.* 2015;31: 199–215.

377 [31] W. Nian, W. Limei, L. Libing, L. Guocheng. Organic intercalation of structure modified  
378 vermiculite. *J Colloid Interf Sci.* 2015;457:264–271.

379 [32] W. Yang, Y. Zheng, A. Zaoui. Swelling and diffusion behaviour of Na-vermiculite at different  
380 hydrated states. *Solid State Ionics.* 2015; 282: 13–17.

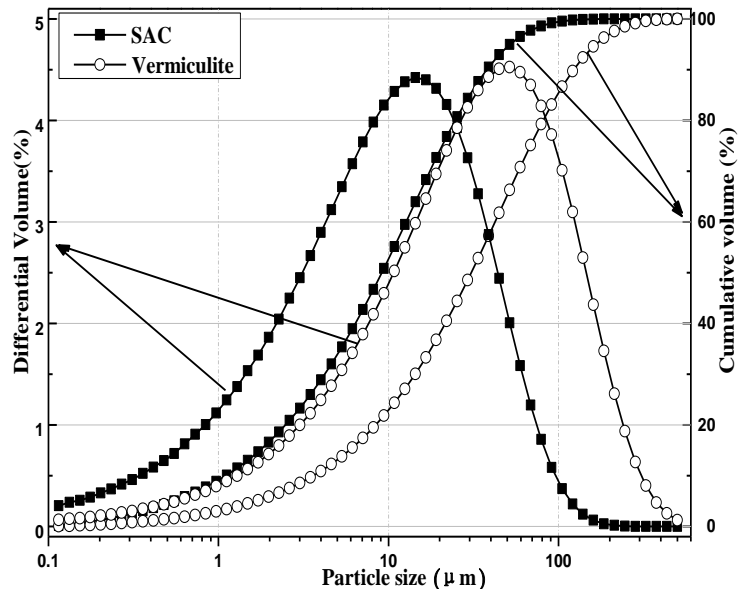
381 [33] C. Marcos, I. Rodríguez. Expansion behaviour of commercial vermiculites at 1000 °C. *Appl Clay*  
382 *Sci.* 2010;48:492–498.

383 [34] D. Jaroslaw, L. Bowen, et al. Vermiculite decorated with copper nanoparticles: Novel antibacterial  
384 hybrid material. *Appl Surf Sci.* 2011;257:9435– 9443.

385 [35] E. E. Alberts, W. C. Moldenhauer. Nitrogen and phosphorus transported by eroded soil aggregates.  
386 *Soil Sci Soc Am J.* 1981; 45(2):391-396.

387 [36] X. Li, Z. Zhang, J. Yang, G. Zhang, B. Wang. Study on the nutrition loss in subsurface runoff  
388 under different ecological measures on red soil slope. *J Water Res & Water Eng.* 2010;21(2): 83-86. (in  
389 Chinese)

- 390 [37]GB (2006) GB/T 20472-2006: Sulfoaluminate cement. Standardization Administration of the  
391 People's Republic of China, Beijing, China. (in Chinese)
- 392 [38] GB (2010) GB/T 2441.1-2010: Determination of urea-Spectrophotometry method. Standardization  
393 Administration of the People's Republic of China, Beijing, China. (in Chinese)
- 394 [39] L. Li, J. Nam, H. H. William. Ex situ leaching measurement of concrete alkalinity. *Cem Concr Res.*  
395 2005;35(2):277–283.
- 396 [40] E. Vejmelková, D. Koňáková, et al. Engineering properties of concrete containing natural zeolite  
397 as supplementary cementitious material: Strength, toughness, durability, and hygrothermal performance.  
398 *Cem Concr Comp.* 2015; 55:259-267.
- 399 [41] S. Roels, J. Carmeliet, et al. Inter laboratory comparison of hygric properties of porous building  
400 materials. *J Therm Envelope Build Sci.* 2004;27: 307–25.
- 401 [42] M. Codina, C. C. Coumes, et al. Design and characterization of low-heat and low-alkalinity  
402 cements. *Cem Concr Res.* 2008;38(4):437–448.
- 403 [43] W. Yongqi, Y. Wu, X. Xiaoming, W. Manjian. Quantitative evaluation of hydrated cement  
404 modified by silica fume using QXRD, <sup>27</sup>Al MAS NMR, TG–DSC and selective dissolution techniques.  
405 *Constr and Build Mater.* 2012;36:925–932.



407

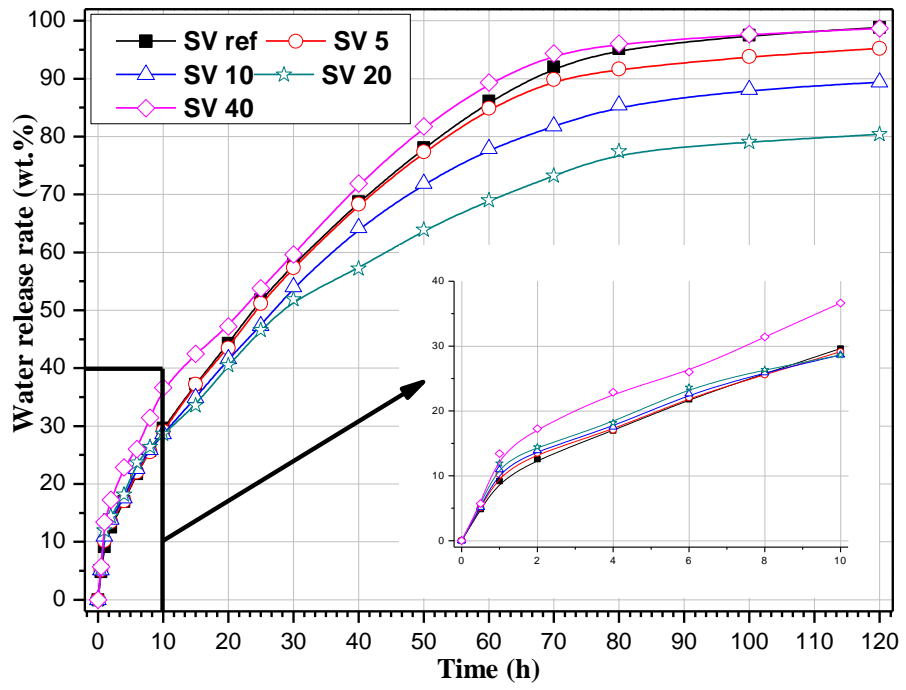
408

409

410

Fig.1 Particle size distributions of SAC and vermiculite

411 Fig.2

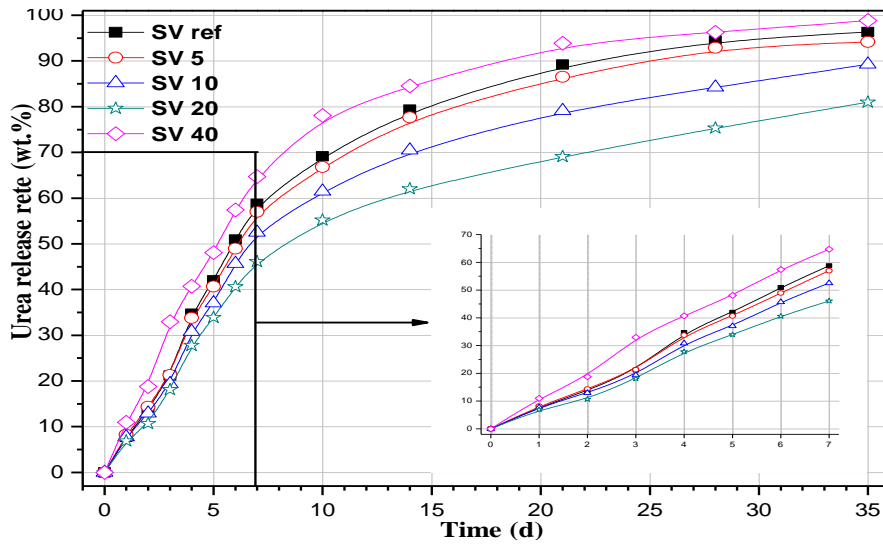


412

413

Fig.2 Water release rate of hardened pastes

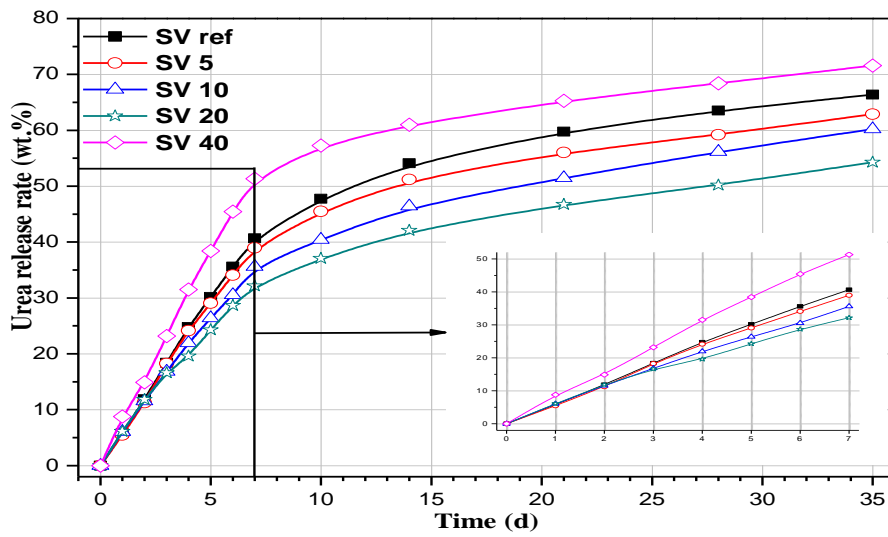




(a) Fertilizer dosage of 2 wt. %

415

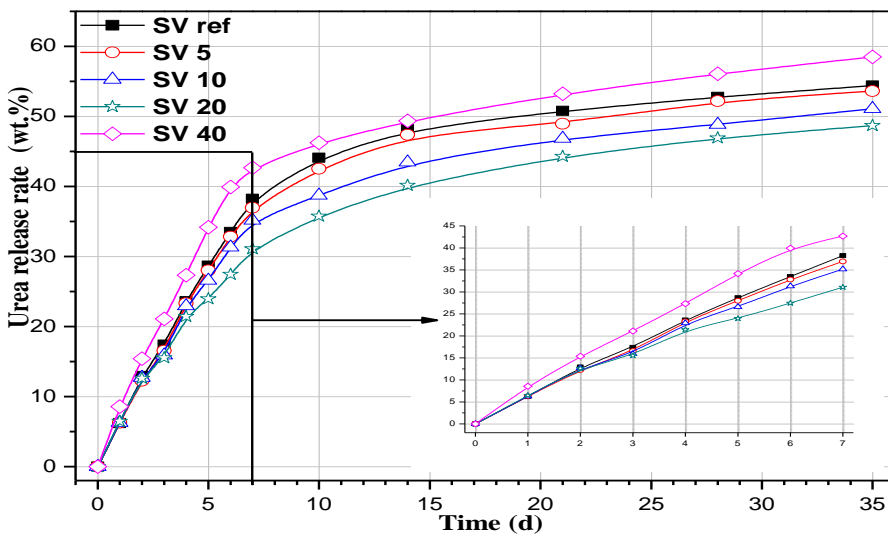
416



(b) Fertilizer dosage of 4 wt. %

417

418



(c) Fertilizer dosage of 8 wt. %

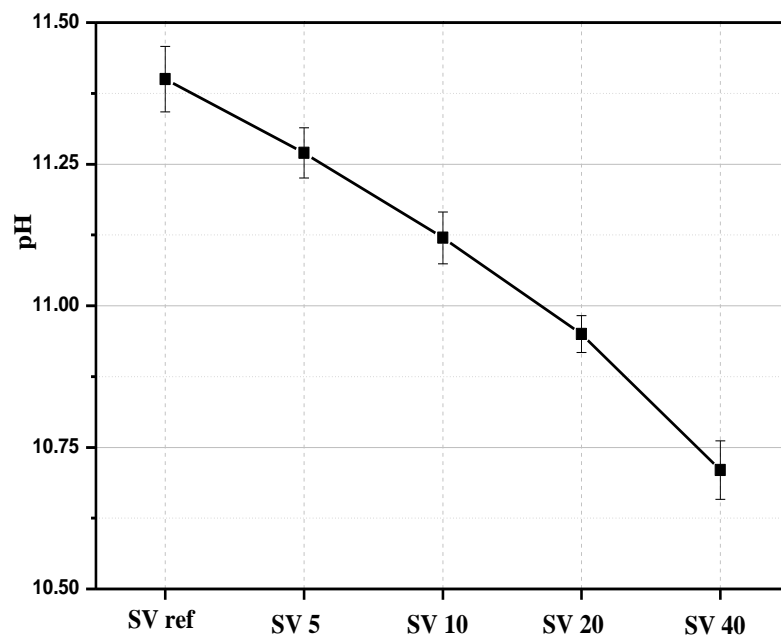
419

420

421

Fig.3 Fertilizer release rate of hardened pastes

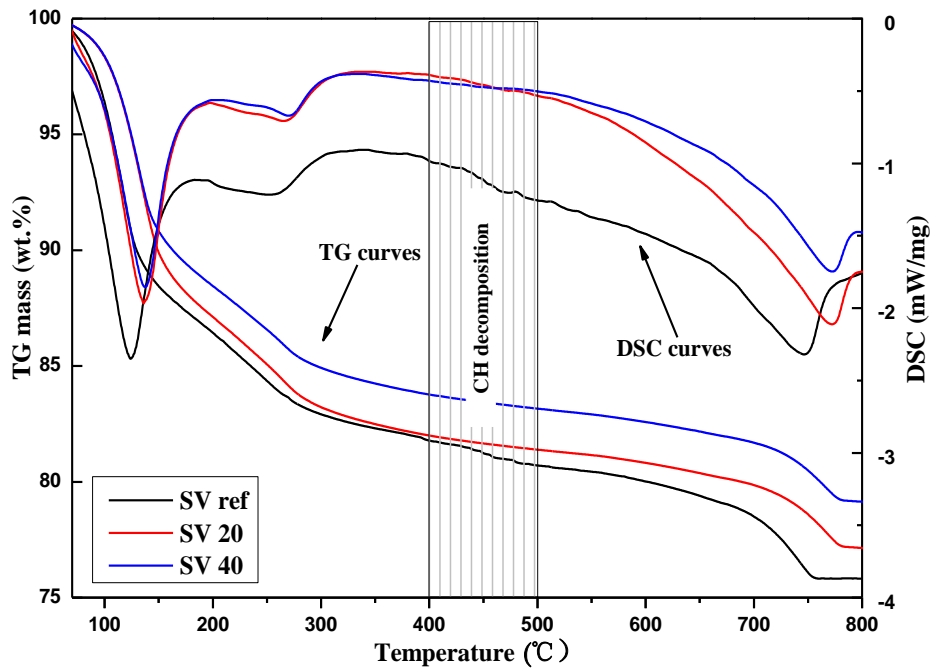
422 Fig.4



423

424

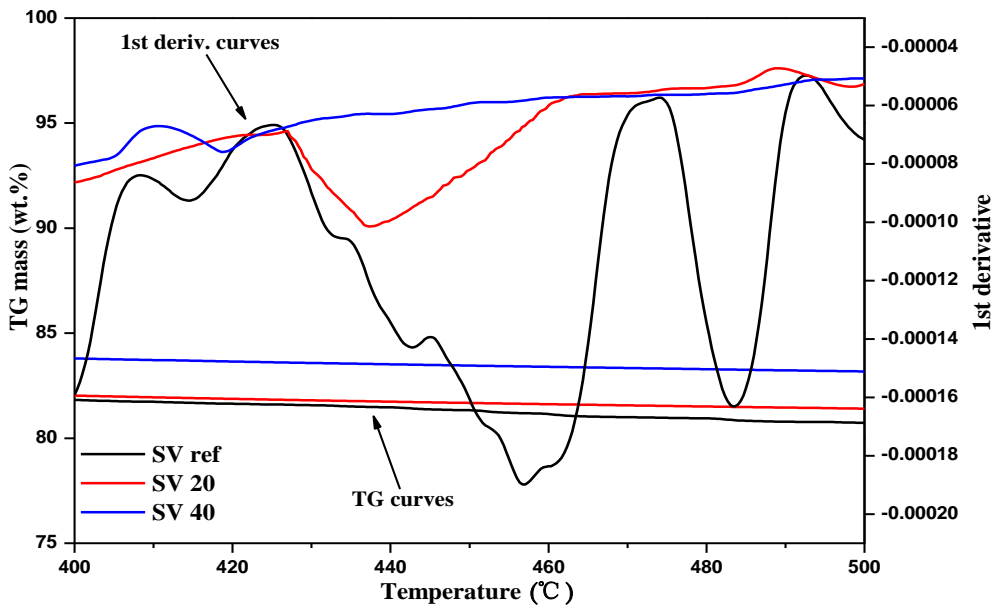
Fig.4 Alkalinity of pore fluid of hardened pastes



426

427

(a) TG-DSC curves



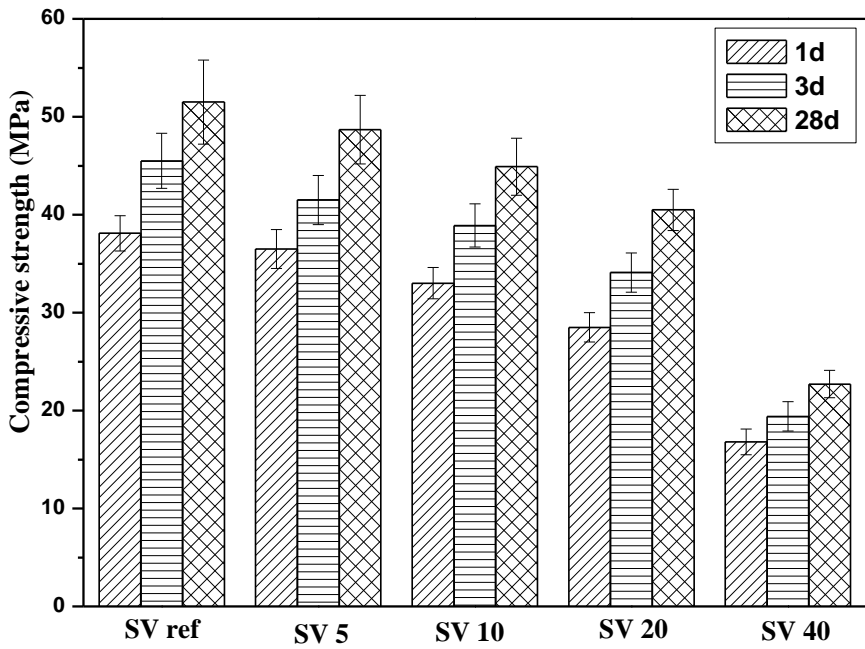
428

429

(b) TG-1st curves

430

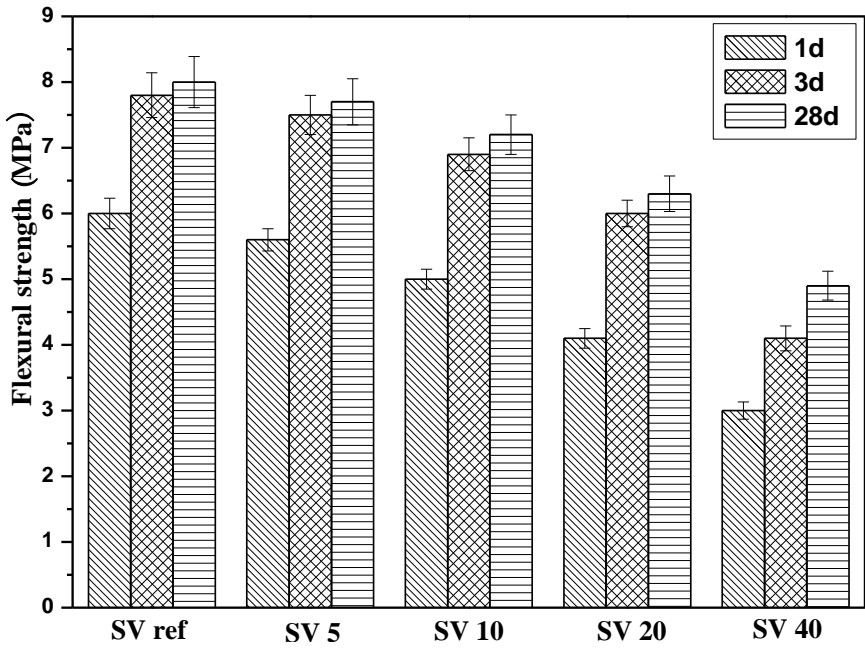
Fig. 5 TG-DSC analysis



432

433

(a) Compressive strength



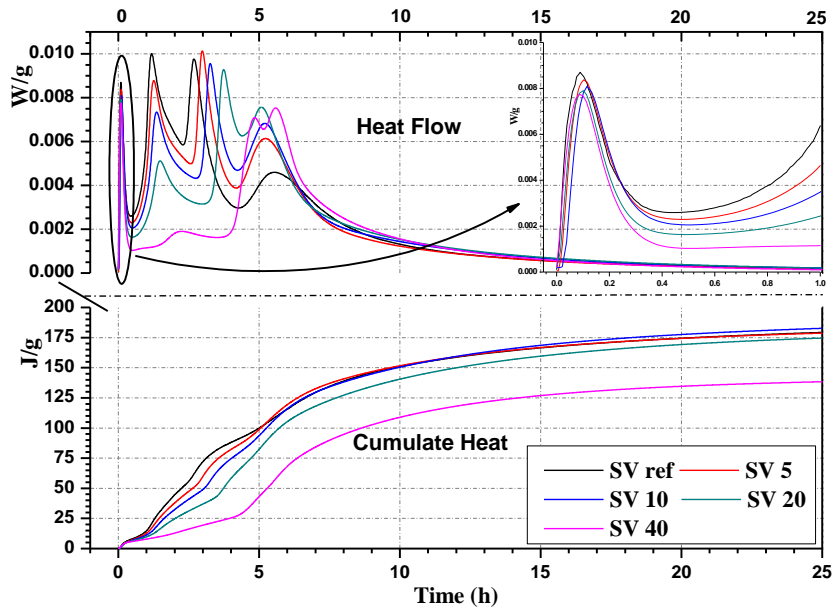
434

435

(b) Flexural strength

436

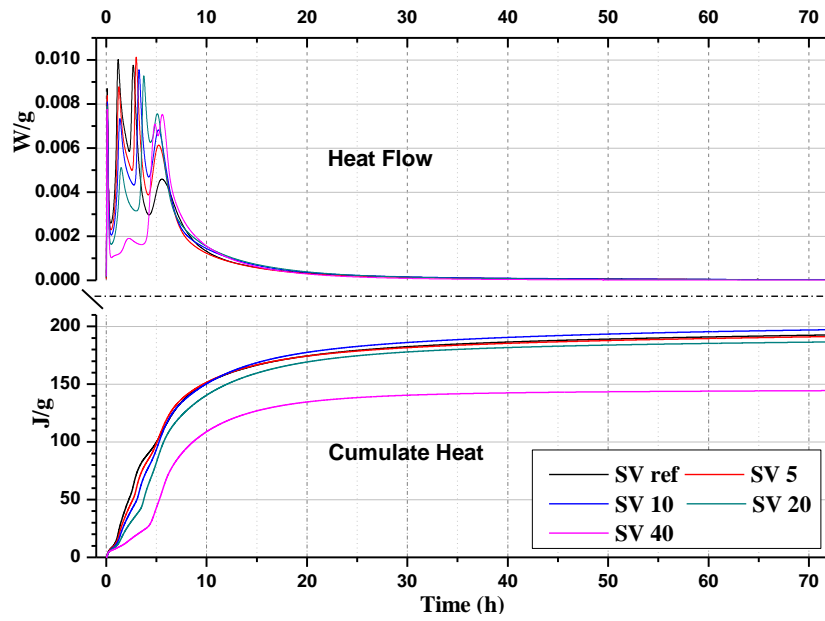
Fig.6 Mechanical properties of cementitious materials



438

439

(a) hydration heat evolution for 1d



440

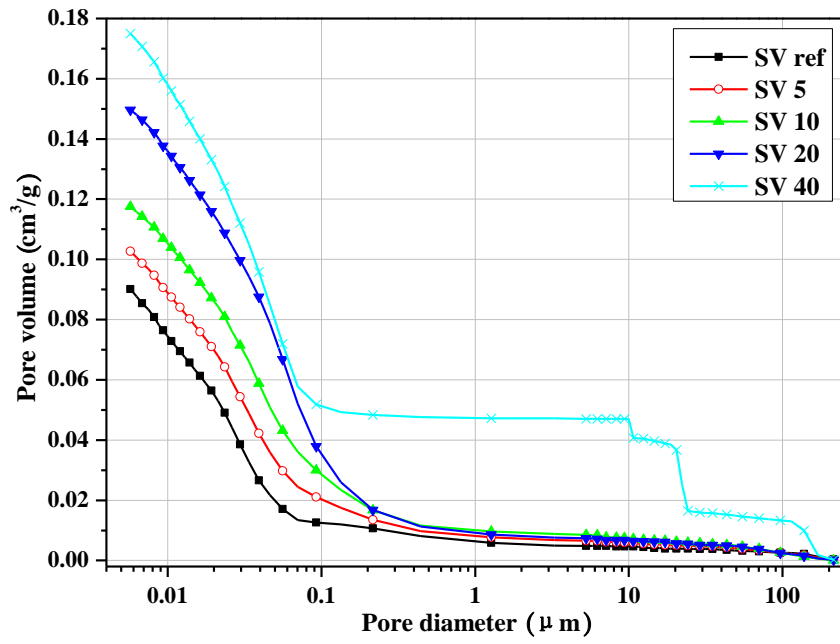
441

442

(b) Hydration heat evolution for 3d

Fig.7 Hydration heat evolution

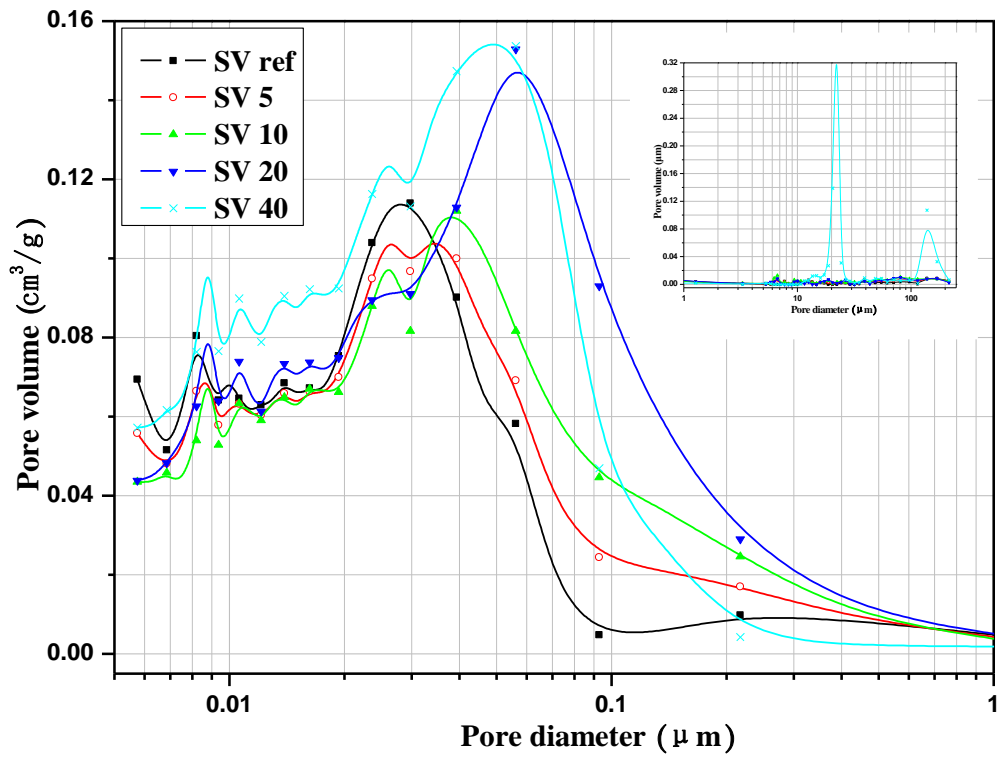
443 Fig.8



444

445

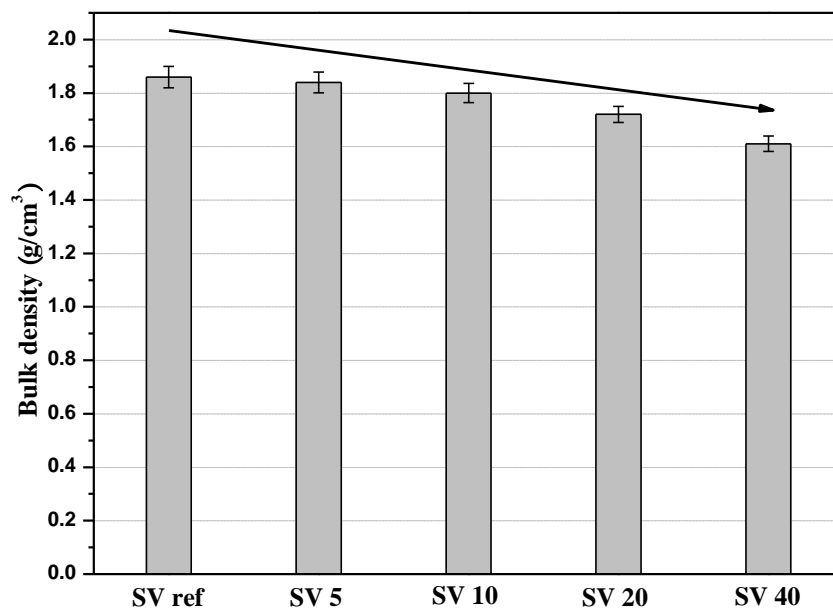
Fig.8 Cumulative pore volume of hardened pastes



447

448

Fig.9 Pore size distribution of hardened pastes



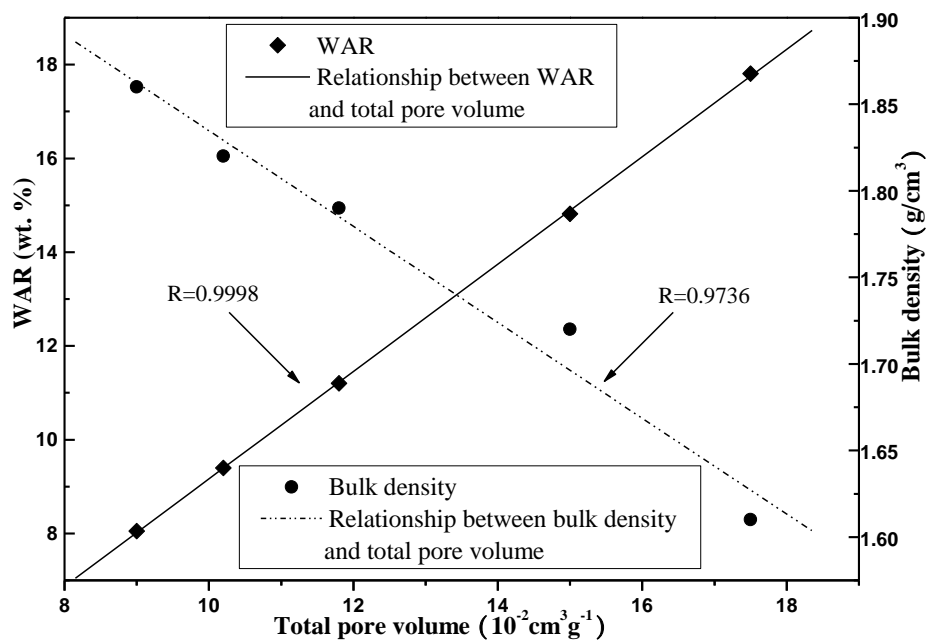
450

451

Fig.10 Bulk density of hardened pastes



452 Fig.11



453

454

455

Fig.11 Relationship between total pore volume and WAR, bulk density

456 **Table 1**

457

**Table 1** chemical composition of SAC and vermiculite

Component	Amount (wt.%)	
	SAC	Vermiculite
SiO <sub>2</sub>	9.16	41.00
CaO	44.37	1.82
Al <sub>2</sub> O <sub>3</sub>	23.26	15.10
Fe <sub>2</sub> O <sub>3</sub>	2.53	16.14
MgO	1.59	12.53
K <sub>2</sub> O	0.44	5.14
Na <sub>2</sub> O	0.29	0.48
TiO <sub>2</sub>	1.01	1.91
SO <sub>3</sub>	10.11	0.08
Ignition loss	6.24	3.20

458

**Table 2** Mix proportions of SAC control sample and samples with additions of vermiculite

No.	Composition (wt. %)	
	SAC	Vermiculite
SV ref	100	0
SV 5	95	5
SV 10	90	10
SV 20	80	20
SV 40	60	40

460

461

462 **Table 3**

463

464

Table 3 WARs of hardened pastes (wt. %)

No.	SV ref	SV 5	SV 10	SV 20	SV 40
WAR	8.05	9.40	11.20	14.82	17.81

465

466